



OPEN ACCESS

EDITED BY

Darko Bosnakovski,
University of Minnesota, United States

REVIEWED BY

Elen H. Miyabara,
University of São Paulo, Brazil
Karim Azzag,
University of Minnesota Medical Center,
United States

*CORRESPONDENCE

Yan Zhao,
✉ doctoryanzhao@whu.edu.cn
Gang Li,
✉ whu_ligang@whu.edu.cn

[†]These authors have contributed equally to this work and share first authorship

RECEIVED 18 February 2024

ACCEPTED 23 April 2024

PUBLISHED 09 May 2024

CITATION

Xing R, Yu H, Yu J, Zeng R, Xiang Z, Ma H, Li G and Zhao Y (2024), Identification of key genes affecting ventilator-induced diaphragmatic dysfunction in diabetic mice.
Front. Genet. 15:1387688.
doi: 10.3389/fgene.2024.1387688

COPYRIGHT

© 2024 Xing, Yu, Yu, Zeng, Xiang, Ma, Li and Zhao. This is an open-access article distributed under the terms of the [Creative Commons Attribution License \(CC BY\)](https://creativecommons.org/licenses/by/4.0/). The use, distribution or reproduction in other forums is permitted, provided the original author(s) and the copyright owner(s) are credited and that the original publication in this journal is cited, in accordance with accepted academic practice. No use, distribution or reproduction is permitted which does not comply with these terms.

Identification of key genes affecting ventilator-induced diaphragmatic dysfunction in diabetic mice

Rongchun Xing^{1,2†}, Haibo Yu^{1†}, Jiangtao Yu¹, Rong Zeng¹, Zhijun Xiang¹, Haoli Ma^{3,4}, Gang Li^{3,4*} and Yan Zhao^{1,5*}

¹Emergency Center, Zhongnan Hospital of Wuhan University, Wuhan, Hubei, China, ²The First College of Clinical Medical Science, Three Gorges University, Yichang, China, ³Department of Biological Repositories, Zhongnan Hospital of Wuhan University, Wuhan, China, ⁴Yichang Central People's Hospital, Yichang, Hubei, China, ⁵Hubei Clinical Research Center for Emergency and Resuscitation, Zhongnan Hospital of Wuhan University, Wuhan, Hubei, China

Background: Mechanical ventilation (MV) is often required in critically ill patients. However, prolonged mechanical ventilation can lead to Ventilator-induced diaphragmatic dysfunction (VIDD), resulting in difficulty in extubation after tracheal intubation, prolonged ICU stay, and increased mortality. At present, the incidence of diabetes is high in the world, and the prognosis of diabetic patients with mechanical ventilation is generally poor. Therefore, the role of diabetes in the development of VIDD needs to be discovered.

Methods: MV modeling was performed on C57 mice and DB mice, and the control group was set up in each group. After 12 h of mechanical ventilation, the muscle strength of the diaphragm was measured, and the muscle fiber immunofluorescence staining was used to verify the successful establishment of the MV model. RNA sequencing (RNA-seq) method was used to detect mRNA expression levels of the diaphragms of each group, and then differential expressed gene analysis, Heatmap analysis, WGCNA analysis, Venn analysis, GO and KEGG enrichment analysis were performed. qRT-PCR was used to verify the expression of the selected mRNAs.

Results: Our results showed that, compared with C57 control mice, the muscle strength and muscle fiber cross-sectional area of mice after mechanical ventilation decreased, and DB mice showed more obvious in this respect. RNA-seq showed that these differential expressed (DE) mRNAs were mainly related to genes such as extracellular matrix, collagen, elastic fiber and Fbxo32. GO and KEGG enrichment analysis showed that the signaling pathways associated with diabetes were mainly as follows: extracellular matrix (ECM), protein digestion and absorption, PI3K-Akt signaling pathway, calcium signaling pathway, MAPK signaling pathway and AGE-RAGE signaling pathway in diabetic complications, etc. ECM has the closest relationship with VIDD in diabetic mice. The key genes determined by WGCNA and Venn analysis were validated by quantitative real-time polymerase chain reaction (qRT-PCR), which exhibited trends similar to those observed by RNA-seq.

Conclusion: VIDD can be aggravated in diabetic environment. This study provides new evidence for mRNA changes after mechanical ventilation in diabetic mice, suggesting that ECM and collagen may play an important role

in the pathophysiological mechanism and progression of VIDD in diabetic mice, and provides some clues for the research, diagnosis, and treatment of VIDD in diabetic context.

KEYWORDS

mechanical ventilation (MV), ventilator-induced diaphragmatic dysfunction (VIDD), diabetes, RNA-seq, mRNA

1 Background

Mechanical ventilation (MV) can maintain alveolar ventilation, increase lung volume, maintain oxygenation, and reduce respiratory work, which is a life-saving measure. However, long-term mechanical ventilation can lead to ventilator-induced diaphragmatic dysfunction (VIDD), which is manifested as diaphragmatic atrophy, decreased contractile force and progressive aggravation, and difficulty in exiting ventilator, which is closely related to poor clinical prognosis (Decramer and Gayan-Ramirez, 2004).

Diabetes is one of the most common metabolic diseases, with a high incidence worldwide, and the prevalence of type 2 diabetes is increasing alarmingly worldwide, with explosive increases in low-income countries and among adolescents/young adults, and with serious implications for longevity and quality of life. The diagnosis, prevention and treatment of the disease face great challenges (Saeedi et al., 2019; Izzo et al., 2021). Clinically, some critically ill patients often need mechanical ventilation. If these critically ill patients have diabetes combined with mechanical ventilation, the prognosis is generally poor, and many studies have shown that diabetes can cause diaphragmatic dysfunction (Van Lunteren and Moyer, 2013). Existing studies on the mechanisms of diabetes-induced muscle damage mostly focus on mitochondrial oxidative stress (Yan et al., 2011; Anderson, 2015). Diabetes may be an important factor in aggravating VIDD. However, previous studies on VIDD models were mostly based on wild-type healthy mouse or rat MV models (Azuelos et al., 2015; Ichinoseki-Sekine et al., 2021; Nakai et al., 2023), and the current omics studies were mostly focused on rat models (Liu et al., 2021a). So far, there has been no study on transcriptomic analysis of diaphragm in MV model of diabetic mice.

In order to understand the changes in mRNA levels caused by mechanical ventilation in patients with diabetes, we used a unique experimental ICU model. Firstly, BKS-DB (DB) mice were selected as the diabetes model (BKS-DB mice were severely obese with significant and continuous glucose increase after *Lepr* gene was knocked out on C57BL/6JGpt mice. Islet atrophy, which may be accompanied by diabetic nephropathy, diabetic retinopathy, and other symptoms). Studies have shown that diaphragmatic dysfunction can occur in mice after 6–12 h of mechanical ventilation, and there is a significant decrease in diaphragmatic contractility after 6 h of mechanical ventilation. After 12 h of ventilation, the diaphragmatic tissue of mice exhibits significant pathological changes and muscle fiber atrophy. Thus, we chose 12 h as the mechanical ventilation time for mice (Picard et al., 2012a; Mrozek et al., 2012; Matecki et al., 2016). Then, BKS-DB diabetic mice were given mechanical ventilation for 12 h and diaphragm mRNA expression levels were detected by high-throughput sequencing, compared with C57BL/6J (C57) control mice. Finally,

we verified the expression of the selected mRNAs using qRT-PCR. We found that mRNA expression changes after MV in diabetic mice, and these changes may shed light on the physiological and pathophysiological processes that occur after MV in diabetic mice, as well as key signaling pathways involved in these genes, which may provide potential therapeutic targets for VIDD.

2 Methods

2.1 Animals

A total of 44 adult SPF (specific pathogen-free) grade male BKS-DB and C57BL/6J mice were obtained from Gempharmatech (Gempharmatech Co., LTD., Chengdu, China). Animal experiments were conducted in the Biosafety Level III Laboratory of Wuhan University (Wuhan, Hubei, China). The mice were kept in cages with the right temperature ($23^{\circ}\text{C} \pm 2^{\circ}\text{C}$) and humidity ($50\% \pm 5\%$), light and dark cycles every 12 h. The mice had free access to water and food. All animal experiments were approved by the Ethics Committee of the Animal Laboratory Center of Zhongnan Hospital of Wuhan University and followed the National Institutes of Health guidelines for the care and use of laboratory animals.

Our manuscript confirming the study is reported in accordance with ARRIVE guidelines. All animal experimental procedures were approved by the Institutional Animal Care and Use Committee of Wuhan University (Number: ZN2021189).

2.2 Establishing mechanical ventilation model

The MV model was established based on the findings reported in several previous articles (Picard et al., 2012a; Mrozek et al., 2012; Matecki et al., 2016). The mice were anesthetized with sodium pentobarbital (50 mg/kg body weight) via intraperitoneal injection and placed on a constant temperature blanket set at 37°C . Mice in the experimental group (MV group) were orally intubated with a 22-gauge angiocatheter and connected to a small animal ventilator (Vent Elite Harvard Apparatus, United States) where a mixture of air and oxygen was heated, humidified, and delivered into the mice's respiratory tracts. Volumetric ventilation mode was adopted with a respiratory rate of 150 times/min, a suction/breathing ratio of 1:1, a tidal volume of 8 mL/kg, and mechanical ventilation for 12 h. Mice in the control group, subjected to sham surgery, maintained spontaneous respiration. After 12 h of mechanical ventilation, the mice were euthanized by intraperitoneal injection pentobarbital sodium (150 mg/kg), and the diaphragmatic tissue was taken

after the mice were completely unconscious, and 5 diaphragmatic muscle specimens from each group were collected and stored at -80°C for RNA-seq analysis. In addition, six mice were sampled from each group, and a portion of each mouse was used to measure the muscle strength of the diaphragm. The remaining part was stored in muscle fixating fluid and used for fast and slow muscle immunofluorescence analysis.

2.3 Measurement of diaphragmatic muscle strength

Take the diaphragm muscle strip (4–6 mm in length and 3–4 mm in width) and quickly immersed it in a constant temperature water bath of Krebs-Henseleit (25°C , pH 7.4) solution. Maintain a continuous supply of a gas mixture consisting of 95% oxygen and 5% carbon dioxide into the water bath. The muscle strip was connected to the muscle force receptor, and the voltage was set to 12 V. Initially, the muscle strip was stimulated with a low frequency (20 Hz), and the baseline was adjusted to find the optimal initial length (cm) of the muscle strip. Subsequently, the diaphragm muscle strips were stimulated with different frequencies (20 Hz, 40 Hz, 80 Hz and 120 Hz), and the corresponding muscle contraction force following stimulation at each frequency was measured. At the end, the weight of the muscle strip is determined in grams (g). Using a muscle density of $1.06\text{ (g/cm}^3\text{)}$, calculate the cross-sectional area (cm^2) of each muscle strip as follows: the optimal initial length = wet weight (g)/density (g/cm^3)/muscle strip length (cm). Finally, the ultimate muscle force (F) of each mouse's diaphragm was standardized as: contractile force (g)/cross-sectional area (cm^2).

2.4 Immunofluorescence staining

Immunofluorescence staining of diaphragm tissue was performed to assess the cross-sectional areas (CSAs) of muscle fibers. The diaphragm specimen was extracted from the animal and fixed using an environmentally friendly muscle fixation solution (Servicebio, Wuhan, China). The diaphragm tissue was embedded in paraffin wax and then transverse sliced with a paraffin microtome (RM 2016, Leica Instrument Co., LTD., Shanghai, China). An environmentally friendly dewaxing solution (Servicebio, Wuhan, China) was used for dewaxing. After washing, the antigen was extracted with EDTA repair solution and washed 3 times with PBS. The slices were put into 3% hydrogen peroxide solution, incubated at room temperature for 25 min away from light, blocked endogenous peroxidase, and then washed with PBS for 3 times. Sections were incubated overnight with mouse anti-fast myosin heavy chain antibodies (Servicebio, Wuhan, China) and anti-slow myosin heavy chain antibodies (Servicebio, Wuhan, China) at 4°C . Then the corresponding second antibody were applied, and the sections were incubated at room temperature for 50 min, followed by a TBST wash. After slightly dried, the slices were used for DAPI staining analysis, and finally the slices were sealed with anti-fluorescence quenching agent (Servicebio, Wuhan, China). Images were captured using the microscope (OLYMPUS IX73, Olympus Co., Japan) and cellSens standard software. The determination of CSAs was performed using Image J software (V1.52a, National Institutes of Health, United States).

2.5 Analysis of RNA sequencing data

In each of the DB-CON, DB-MV, C57-CON, and C57-MV groups, five samples of diaphragmatic tissue were collected. Total RNA was extracted from diaphragm tissue with TRIzol reagent (Invitrogen, Carlsbad, CA, United States) as recommended in the instructions and genomic DNA was removed using DNase I (TaKara, Beijing, China). The purity and integrity of the RNA were assessed using the NanoDrop (Thermo Fisher) and Bioanalyzer 2100 systems (Agilent Technologies, United States). RNA-seq transcriptome library was prepared following TruSeq RNA sample preparation Kit from Illumina (San Diego, CA) with $1\text{ }\mu\text{g}$ of total RNA for each. The raw paired end reads were trimmed and quality controlled by SeqPrep and Sickle with default parameters. Reference genome and gene model annotation files were downloaded directly from the genome website. Alignment to the Reference genome was performed using Hisat2 (v2.0.1). The mapped reads of each sample were assembled and quantified gene abundances by StringTie. To identify DEGs (differential expressed genes) between two groups, the expression level of each transcript was calculated according to the transcripts per million reads (TPM) method. The differentially expressed mRNA was identified with R-package DESeq2 by $|\log_2(\text{fold change})| > 0.58$ and $p\text{-value} < 0.05$. Then differential gene statistical analysis, heatmap analysis, WGCNA analysis, Venn analysis, GO and KEGG enrichment analysis were performed.

2.6 Quantitative real-time polymerase chain reaction verification in VIDD mice

The expression levels of 15 most critical genes (Eln, Mfap5, Pcolce, Fbn1, Fstl1, CD248, Col1a1, Col1a2, Col3a1, Col5a1, Col6a1, Col6a2, Col6a3, Col15a1, Fbxo32) selected by the analysis of RNA-seq were validated by qRT-PCR using three samples in each of the four groups. Total RNA was extracted from diaphragm tissue using a mirVana miRNA Isolation Kit (Ambion, Austin, TX, United States) according to the manufacturer's protocol, and the concentration and purity were assayed using a NanoDrop spectrometer (Thermo Fisher Scientific, Inc.). A total of $1\text{ }\mu\text{g}$ of total RNA was used to synthesize cDNA using a ReverTra Ace qPCR RT Kit (cat. no. FSQ-101; Toyobo Life Science, Osaka, Japan; Code No. FSQ-101). The RNA samples were mixed with RT kit reagents and incubated at 37°C for 15 min and 99°C for 5 min. Finally, the samples were diluted in diethylpyrocarbonate-treated water and stored at -20°C . cDNA was amplified and recorded using SYBR Green Real-Time PCR Master Mix (cat. no. QPK-201; Toyobo Life Science) on a CFX Connect Real-Time PCR System (Bio-Rad; CFX Maestro 1.0 software). All primers were synthesized by Genscript Biotech Corporation, Inc., and the sequences are shown in [Supplementary Table S1](#). The expression of the selected mRNAs was normalized to that of the housekeeping gene GAPDH. The thermocycling program for PCR consisted of 40 cycles of 5 s at 95°C , 10 s at 55°C , and 15 s at 72°C , followed by a final extension at 72°C for 5 min and a melt curve analysis from 65°C to 95°C . The data were analyzed using the $2^{-\Delta\Delta\text{CT}}$ method (Schmittgen and Livak, 2008).

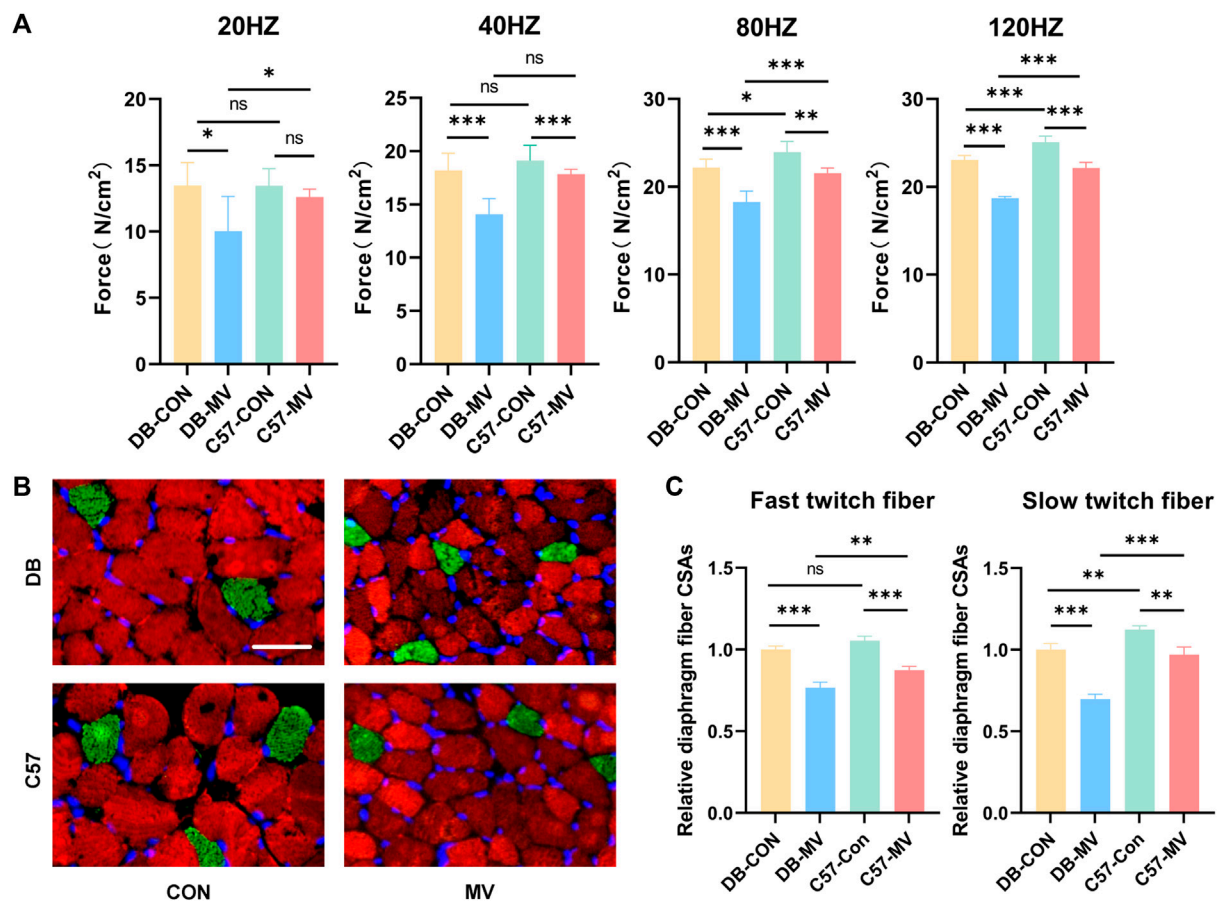


FIGURE 1

The changes of diaphragmatic muscle strength, immunofluorescence staining images and relative diaphragmatic cross-sectional area of mice in each group after mechanical ventilation were stimulated at different frequencies. (A) Changes of muscle strength of diaphragm under different frequency stimulation ($n = 6$ in each group); (B) Representative immunofluorescence staining of fast-twitch fibers (red) and slow-twitch fibers (green) in diaphragmatic cross-sectional area in each group ($n = 3$ in each group), scale bar, 50 μm ; (C) Comparison of changes in relative diaphragmatic cross-sectional area after mechanical ventilation in DB and C57 mice. The relative cross-sectional area of each group was normalized by the DB-CON group. Scale bar = 50 μm . Groups: DB-CON, DB-control group; DB-MV, DB-mechanical ventilation group; C57-CON, C57-control group; C57-MV, C57-mechanical ventilation group. *, ** and *** are separately indicates p -values < 0.05, 0.01 and 0.001. The error bars indicate the \pm SD.

2.7 Statistical analysis

In addition to transcriptome data, the data of diaphragm muscle strength and muscle fiber cross-sectional area were showed as mean \pm standard deviation (SD). Student's t tests were used for comparisons between two groups. The data were analyzed using Prism software (v8.0.1, SanDiego, United States), and p -value < 0.05 was considered significant.

3 Results

3.1 Diaphragmatic muscle strength measurement

The diaphragmatic muscle strength of DB and C57 mice in MV group and control group were compared under different frequency stimulation (20 HZ, 40 HZ, 80 HZ and 120 HZ). The diaphragmatic

muscle strength of DB and C57 mice decreased after mechanical ventilation compared with their respective controls (Figure 1A). Compared with C57 mice, DB mice experienced a more significant decrease in diaphragmatic muscle strength after mechanical ventilation (Figure 1A).

3.2 Diaphragm immunofluorescence results

The cross-sectional area of diaphragmatic fibers in DB and C57 mice was compared between MV group and control group. The transverse area of the diaphragm fibers in both DB and C57 mice decreased after mechanical ventilation compared to the control group (Figures 1B, C). Compared with C57 mice, the transverse area of the diaphragm fibers of DB mice was more significantly reduced after mechanical ventilation (Figures 1B, C).

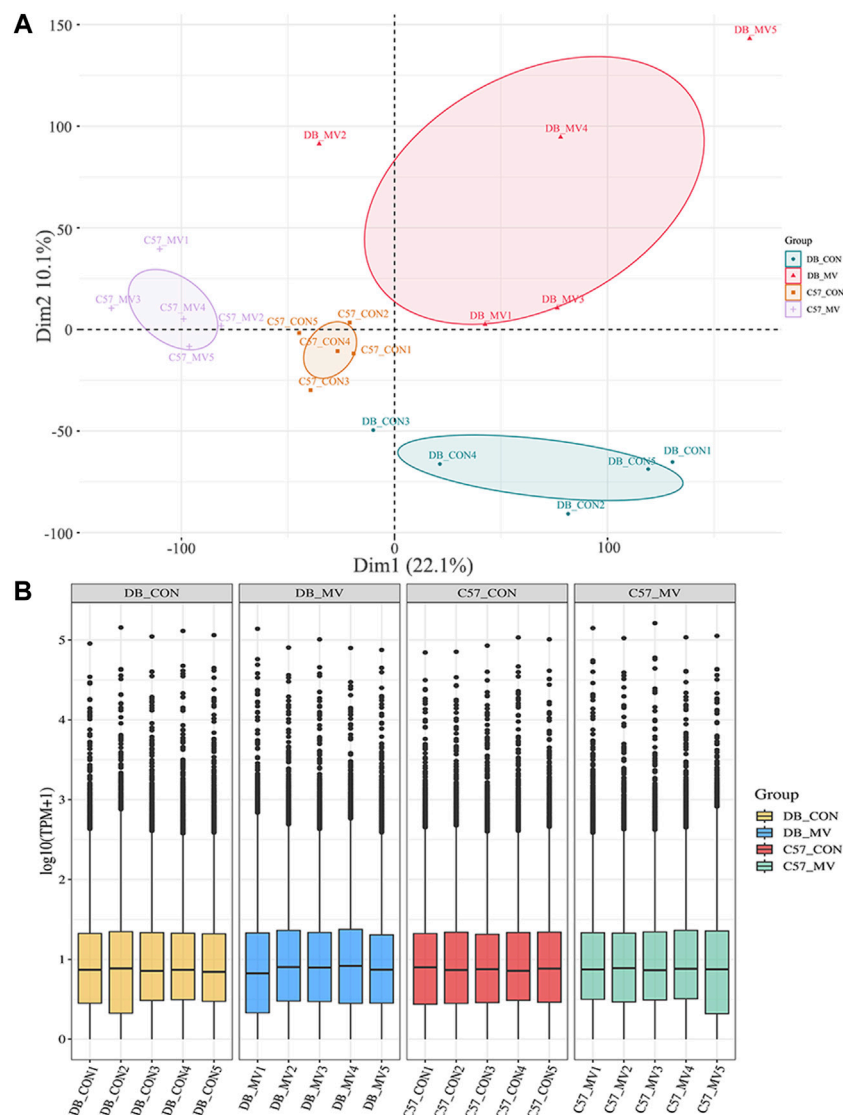


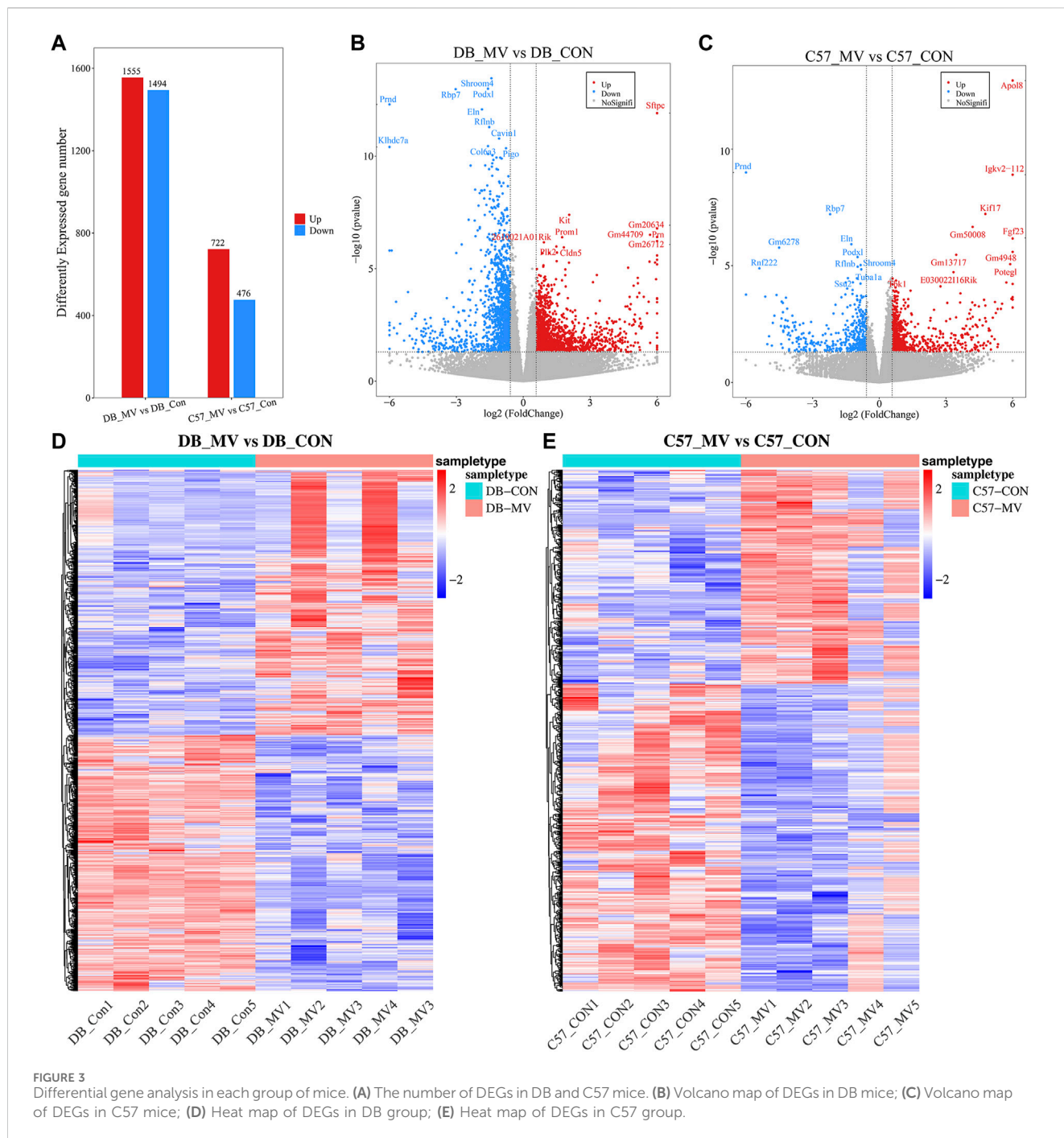
FIGURE 2 Principal component analysis and boxplot of mRNA expression in different groups. **(A)** Principal Component Analysis (PCA) between different groups. **(B)** mRNA expression levels in each group.

3.3 RNA-seq in diaphragm tissue

RNA-seq was used to identify mRNA associated with MV pathophysiological mechanisms and compare the differences in transcription levels between the MV groups of DB and C57 mice and their respective controls. Count and TPM were used as gene expression level (Supplementary Table S2). Principal component analysis (PCA) was performed to test the relationship among four groups of samples (DB-CON group, DB-MV group, C57-CON group, and C57-MV group) (Figures 2A, B). From that, we found that the confidence ovals of the samples in the control group and the MV group were separated from each other. And the result also suggests that the gene expression pattern in the same group was similar, and the difference among different groups was significant. These results show that the MV model has repeatability for VIDD, the reliability of the experiment is acceptable, and it can be further analyzed.

3.4 Analysis of differentially expressed genes and enrichment analysis

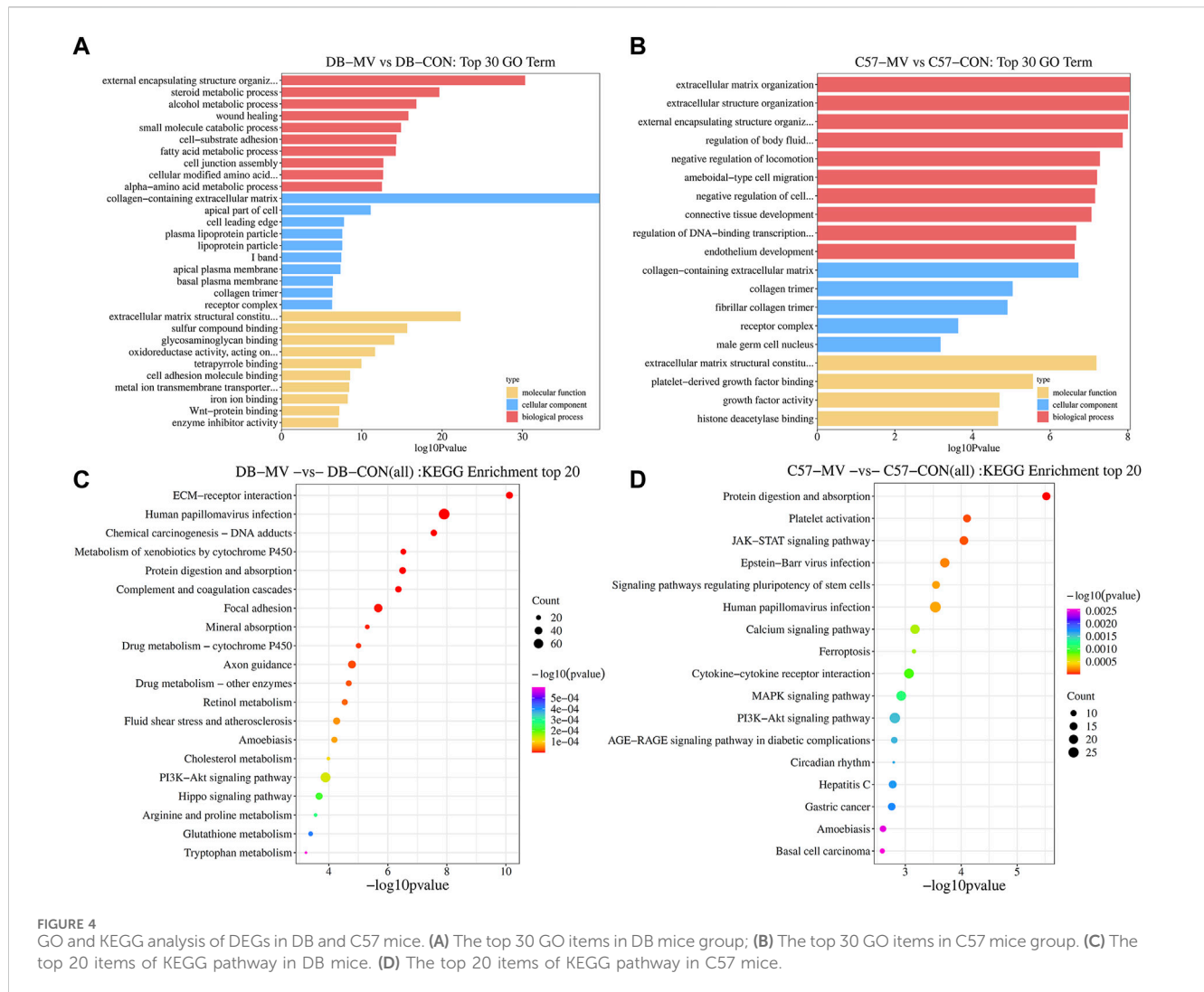
The gene expression of DB and C57 mice in mechanical ventilation group and control group was analyzed. $|\log_2FC| > 0.58$ and $p\text{-value} < 0.05$ were set as threshold for differentially expressed genes (DEGs). A total of 3,049 DEGs were obtained in DB group, including 1,555 upregulated genes and 1,494 downregulated genes. And in the C57 group, a total of 1,198 DEGs were obtained including 722 upregulated genes and 476 downregulated genes (Figure 3A and Supplementary Table S3). Top 20 DEGs with the most significant p -value were shown in volcano maps (Figures 3B, C). The gene expression pattern of all DEGs were shown by heat maps in different groups (Figures 3D, E). In order to understand the function of DEGs in DB and C57 mice after mechanical ventilation compared with the respective control group, the GO and KEGG enrichment



analysis of DEGs in DB and C57 mice were performed and the results showed that ECM, collagen-containing extracellular matrix, protein digestion and absorption, PI3K-Akt signaling pathway, etc., they are important signaling pathway changes in mechanical ventilation (Figures 4A–D and Supplementary Tables S4, S5). By further network analysis of GO and KEGG enriched signaling pathways, we can obtain specific signaling pathways that respond to mechanical ventilation in mice with diabetic background. Such as cell junction assembly, inflammatory mediator regulation of TRP channels, glutathione metabolism, metabolism of xenobiotics by cytochrome P450, relaxin signaling pathway and ECM-receptor interaction, etc. (Figures 5A, B).

3.5 The results of weighted gene co-expression network analysis (WGCNA)

The gene expression profiles of the DB-CON, DB-MV, C57-CON and C57-MV groups were subjected to clustering analysis. To construct a co-expression network, we chose 7 as the lowest power that constructs a scale free topology (Figure 6A). Next, we converted the expression matrix to an adjacency matrix, and then converted it to a topological matrix. The average linkage hierarchical clustering method was used to cluster the genes. We also set the minimum number of genes in each gene network module to 50 according to the criteria of hybrid dynamic shear tree, which was used to identify

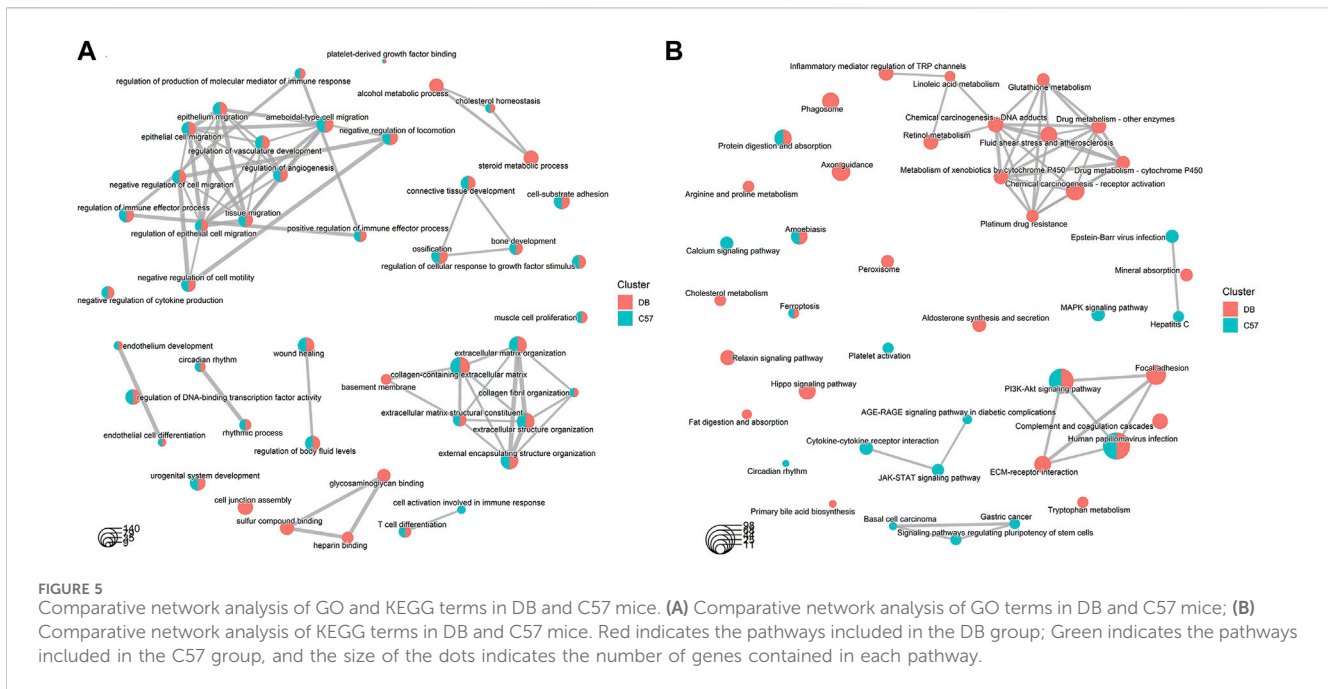


gene modules and calculate the characteristic gene value of each module. The parameters were as follows: height (MEDissThres) = 0.25, depth division = 2, minimum module size = 50; A total of 24 modules were obtained (Figure 6B). The positive and negative correlation modules with the highest correlation with diabetes and mechanical ventilation were selected respectively (positive correlation module darkslateblue, $r = 0.48$, $p = 0.03$; Negative correlation module grey60, $r = -0.67$, $p = 0.001$). The significance of genes in darkslateblue module and grey60 module was $cor = 0.66$, $p = 1.7e-94$, $cor = 0.78$, $p = 1e-200$, respectively (Figures 6C, D). Genes $GS > 0.5$ and $MM > 0.8$ were selected for analysis.

3.6 Identification and enrichment analysis of VIDD key genes in diabetic mice

To identify essential genes function on the regulation of VIDD in diabetic mice, Venn analysis was performed on 3,049 DEGs in DB group, 1,198 DEGs in C57 group, 211 genes of WGCNA darkslateblue module and 25 genes of

grey60 module, and finally, 67 genes were obtained (Figure 7A). Then we constructed a protein interaction network between them (Figure 7B), and the gene expression pattern of the most critical 15 genes was shown by a heat map (Figure 7C). It was found that the differentially expressed genes affecting MV in DB mice were mainly related to collagen, and the closely related collagen proteins were Col1a1, Col1a2, Col3a1, Col5a1, Col6a1, Col6a2, Col6a3, Col8a2 and Col15a1. Compared with C57 mice, the expression levels of some extracellular matrix related genes, such as collagen, elastin Eln, fibrin Fbn1, Mfap5, Pcolce, and CD248, decreased more significantly after mechanical ventilation in DB mice (Figure 7C). In addition, compared with C57 mice, the expression of Fbxo32 gene in the diaphragm of DB mice was more significantly elevated after MV (Figure 7B). GO and KEGG enrichment analysis of the 67 genes showed that the main pathways related to diabetes were extracellular matrix (ECM), protein digestion and absorption, PI3K-Akt signaling pathway, calcium signaling pathway, MAPK signaling pathway and AGE-RAGE signaling pathway in diabetic complications, etc. (Figures 7D, E and Supplementary Table S6), ECM have the closest relationship with VIDD in diabetic mice.



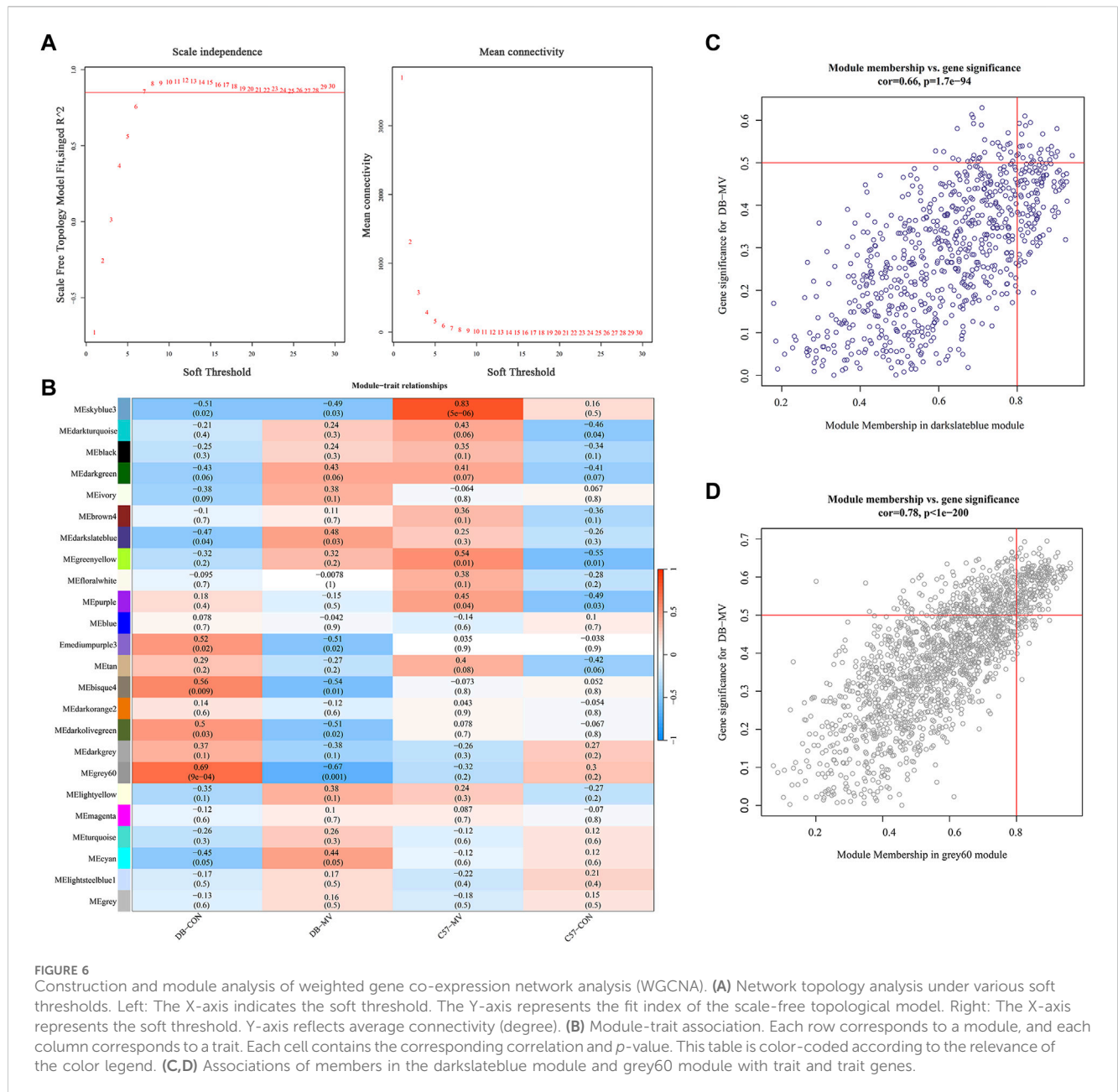
3.7 Quantitative real-time polymerase chain reaction verification

Next, we verified the expression of the 15 most critical genes using qRT-PCR. Comparisons between qRT-PCR results were performed using independent sample Student's t tests. The results showed that compared with C57 mice, the expression of *Fbxo32* in the diaphragm of DB mice was more significantly elevated after MV, while most of the 15 genes' expression levels decreased more significantly after MV in DB mice (Figure 8). Although there were no significant differences in the expression of *Col1a2*, *Col6a1*, etc. between DB and C57 mice, there was a downward trend (Figure 8). In conclusion, the gene expression patterns verified by qRT-PCR were generally consistent with those detected by RNA-seq.

4 Discussion

In this study, we successfully established MV models in DB and C57 mice, which successfully replicated the genotypic and phenotypic characteristics of the diaphragm with impaired function and structure in diabetic mice in the MV state. Compared with mice in the C57 group, we observed significant decrease in diaphragm muscle strength and muscle fiber cross-sectional area after mechanical ventilation in diabetic mice, leading to more severe VIDD. Based on these phenotypic characteristics, we further explored DEGs in MV models of DB and C57 mice, identified key genes associated with diaphragm dysfunction in diabetic mice by WGCNA analysis, and predicted the biological function of DEGs and the signaling pathway which they participate in by GO and KEGG analysis. This may help elucidate the role of genes in the pathophysiology of VIDD in diabetic mice and provide some basis for the study and treatment of VIDD in diabetic patients.

Our study found that the muscle strength of the diaphragm and the cross-sectional area of both fast and slow-twitch fibers decreased after MV in C57 mice (Figures 1A–C), and this was more pronounced in DB mice (Figures 1A–C). Past studies showed that fast-twitch fibers are required for instantaneous exercise and have a high demand for glycolysis, while slow-twitch fibers are necessary for extended periods of exercise and utilize mitochondrial respiration and thus contain abundant mitochondria (Yasuda et al., 2023). Thus, the effect of diabetes on VIDD may be different for different muscle fibers. Wang, Y. etc. showed that disuse-related skeletal muscle atrophy that typically occurs during denervation, immobilization is primarily type I (slow-twitch) fiber-related, whereas nutrient-related atrophy such as cancer/aging cachexia, sepsis, and diabetes are more directed to type II (fast-twitch) fiber wasting (Wang and Pessin, 2013). In our study both types of muscle fibers, fast and slow, were found to be affected in the diaphragm after mechanical ventilation, and there is no significant difference between them. It is probably because oxidative stress impairs both fast and slow muscles. Liu and Li (2018) showed that MV-induced oxidative stress in the diaphragm can impair diaphragm contractility. Another study showed that elevated levels of Reactive Oxygen Species (ROS) in the diaphragm during mechanical ventilation, which in turn causes oxidative stress injury, is a prerequisite for diaphragmatic dysfunction (Zhu and Sassoon, 2012). The diaphragm is a type of striated muscle with specific physiological characteristics that make it more sensitive to events causing oxidative stress compared to other skeletal muscles (Fogarty et al., 2018). Diabetic mice showing more severe diaphragm dysfunction may be due to the higher levels of oxidative stress caused by elevated blood glucose in the mice. Studies have shown that in a model of insulin-dependent diabetes induced by streptozotocin injection (430 vs. 110 mg/dL in the hyperglycemic model and control group), compared with the control group, diaphragmatic muscle mass decreased by one-third and muscle



strength decreased by 40% (Callahan LA and Supinski, 2014; Hafner et al., 2014), which was basically consistent with our findings. Previous studies have found that MV increases oxidative stress levels in the diaphragms of wild-type mice (Picard et al., 2012b). In contrast, our study found that the muscle strength and muscle fiber cross-section area of diabetic mice decreased more significantly after MV, which may be related to the hyperglycemia and oxidative stress environment of diabetic mice. At the cellular level, studies have shown that hyperglycemia can significantly enhance the level of oxidative stress, and oxidative stress can cause the release of mitochondrial ROS, resulting in mitochondrial dysfunction and aggravating diaphragm dysfunction (Leverve, 2003; Callahan LA and Supinski, 2014), indicating that hyperglycemia may lead to the deterioration of VIDD oxidative stress level, and controlling blood glucose level will help improve VIDD in diabetic mice.

To further investigate the transcriptional changes of DB and C57 mice, RNA sequencing was performed on diaphragm samples of each group. Analysis of DEGs combined with WGCNA showed that Fbxo32 (Atrogin-1) expression in the diaphragm increased after mechanical ventilation in C57 mice, and Fbxo32 in the diaphragm of DB mice increased even more (Figure 7B). Studies have shown that Fbxo32, an important transcription factor, is an important marker reflecting muscular atrophy (Liu et al., 2021b). Our previous studies on diaphragmatic in the rat VIDD model also found that the expression of Fbxo32 is upregulated after MV (Liu et al., 2021b), which is consistent with the results of our current study. Fbxo32 increased more significantly in the diaphragm tissue of DB mice after MV, which provided further evidence that MV induced more severe diaphragm dysfunction and atrophy in mice with diabetes versus healthy mice.

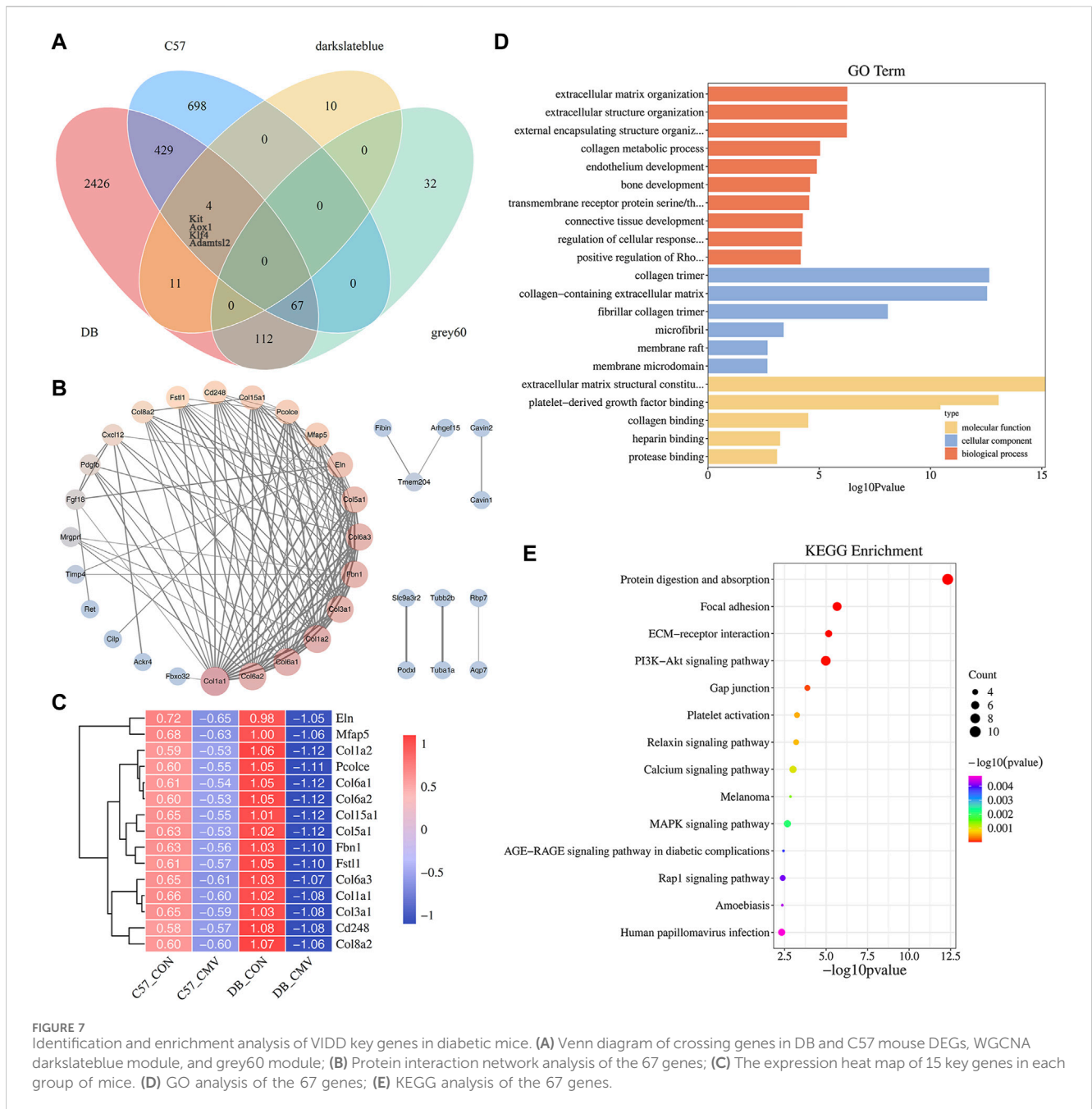


FIGURE 7 Identification and enrichment analysis of VIDD key genes in diabetic mice. (A) Venn diagram of crossing genes in DB and C57 mouse DEGs, WGCNA darkslateblue module, and grey60 module; (B) Protein interaction network analysis of the 67 genes; (C) The expression heat map of 15 key genes in each group of mice. (D) GO analysis of the 67 genes; (E) KEGG analysis of the 67 genes.

In addition, our RNA-seq results found that the differentially expressed genes affecting MV in DB mice were mainly related to collagen, and the closely related collagen were as follows: Col1a1, Col1a2, Col3a1, Col5a1, Col6a1, Col6a2, Col6a3, Col8a2 and Col15a1, and other extracellular matrix related genes such as: elastin Eln, fibrin Fbn1, Mfap5, Pcolce, CD248 and other genes (Figures 7B, C), which decreased more significantly after MV than that in C57 mice (Figures 7B, C), suggesting that these genes may be the key genes affecting VIDD in diabetic mice. We also verified the reliability of their expression by qPCR and found that the mRNA expression levels of most genes in each group were consistent with the RNA-seq sequencing results. The reason for the non-significant difference in expression changes of Col1a2, Col6a1, etc. may be due to the small sample size of mice or the limitation of individual

differences, but the trend of the gene expression levels in each group is generally consistent with the RNA-seq sequencing results, indicating that the results are basically reliable.

Studies have found that collagen is an important part of the extracellular matrix, a key protein for muscle contraction and muscle strength maintenance, and participates in the remodeling of muscle fibers and the maintenance of muscle tone (MAA, 2019). In our study we found that the collagen Col6 family accounted for the highest proportion of the major differential genes, and we predicted that they might play an important role in the diaphragm dysfunction during mechanical ventilation in DB mice. Previous studies have found that type 6 collagen has three genes encoding three main chains: Col6a1, Col6a2, and Col6a3 (Weil et al., 1988; Heiskanen et al., 1995). It is widely expressed in

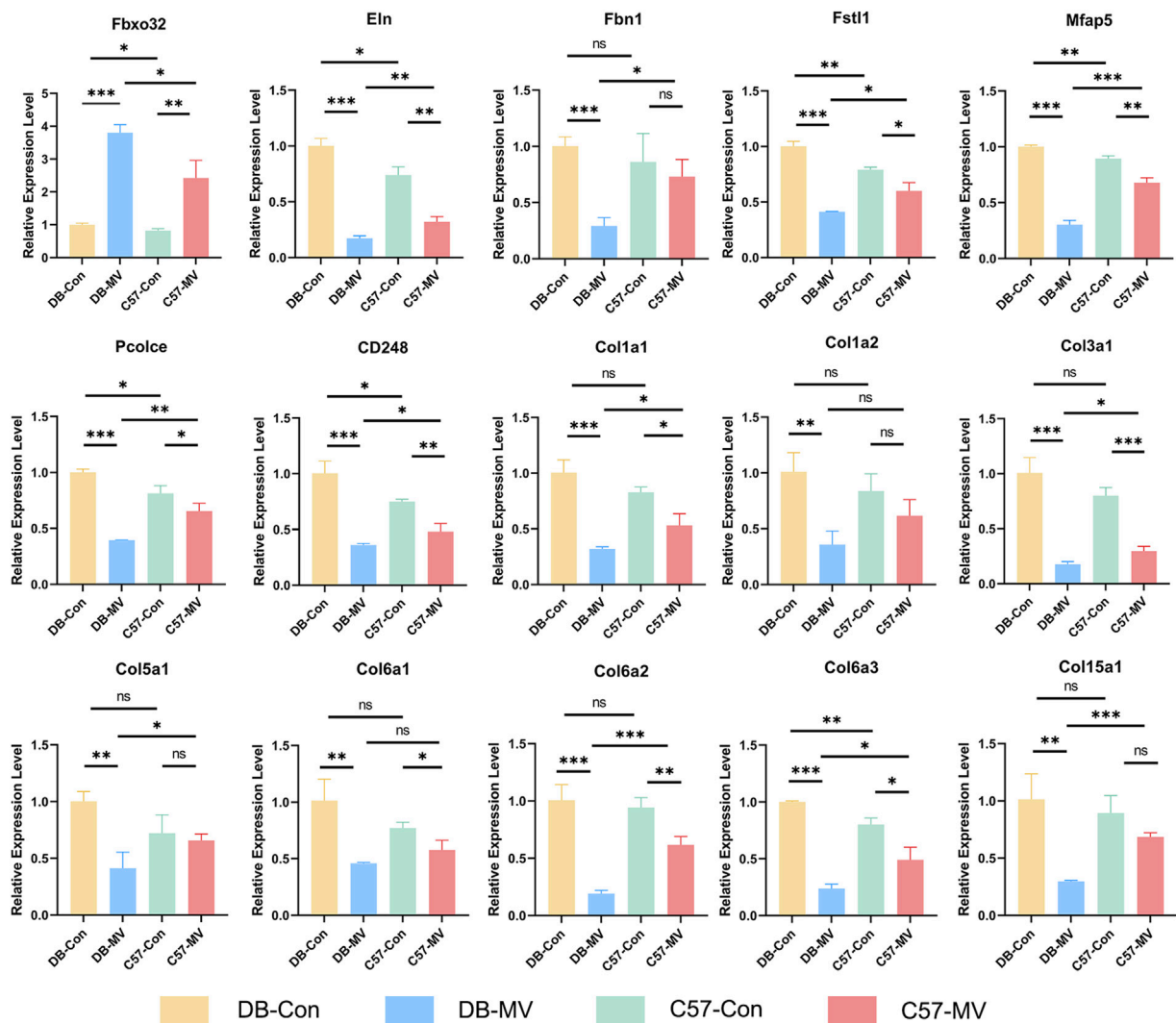


FIGURE 8
Results of qRT-PCR for selected mRNAs in four groups. The relative expression of each mRNA in each group was normalized using the DB-CON group. *, ** and *** are separately indicates p -values < 0.05, 0.01 and 0.001. The error bars indicate the \pm SD.

muscles, tendons and junctions of tendons (Hessle and Engvall, 1984; Keene and Glanville, 1988). Col6 plays a key role in maintaining skeletal muscle cell and tissue homeostasis, mediating muscle fiber anchoring from basal layer to interstitial ECM (Kuo et al., 1997; Lamandé and Bateman, 2018). At the same time, Col6 represents a finely tunable binding platform in ECM, linking several collagens (including types 1, 2, 4, 5, and 14), various glycoproteins, glycosaminoglycans, hyaluronic acid, and heparin, as well as other ECM factors and molecules (Cescon et al., 2015; Castagnaro et al., 2021). In addition, Col6 plays a variety of functions in the tissues in which it is expressed, ranging from mechanical roles (a typical collagen component in ECM) to more specific cellular protective functions (including inhibition of apoptosis and oxidative damage), regulation of cell differentiation and autophagy mechanisms (Cescon et al., 2015). Type 6 collagen, as an ECM protein, is essential for maintaining muscle and skin integrity and function. When the genes encoding their main chains, Col6a1, Col6a2 and Col6a3 are mutated, they cause

congenital muscle disorders. The main manifestations of type VI collagen-related myopathy are hypotonia, muscle weakness, proximal contracture and distal relaxation (Allamand et al., 2010; Di Martino A et al., 2023; Starace et al., 2023). In our study, we found that Col6a1, Col6a2 and Col6a3 are the main differentially expressed genes in the diaphragm of diabetic mice after mechanical ventilation, and they were closely related to each other. The decreased expression may be related to the aggravation of VIDD in diabetic mice.

To further clarify the function of Col6, in the Col6a1^{-/-} mouse model, the absence of the α 1 backbone leads to the complete absence of Col6 secretion in all tissues (Bonaldo et al., 1998). Studies in mice with Col6a1 deletion have shown that Col6 has a protective effect on cells because the deletion of the gene triggers spontaneous apoptosis of muscle fibrocytes, which is associated with potential mitochondrial dysfunction and organelle changes (Irwin et al., 2003). In Col6 knockout muscles, increased mitochondrial intima permeability transition pore (PTP) openings are thought to

contribute to the muscular dystrophy phenotype (Angelin et al., 2007; Bernardi and Bonaldo, 2008). In addition, other studies have shown that the mitochondrial changes in Col6a1^{-/-} mouse muscles are caused by the regulatory defects of the autophagy pathway, and reactivation of the autophagy pathway through drug, genetic or nutritional pathways can rescue the dysfunction of organelles, inhibit apoptosis and prevent the decline of muscle strength (Grumati et al., 2010; Chrisam et al., 2015; Metti et al., 2021). Since the absence of Col6 can lead to muscle dysfunction or muscular atrophy (Di Martino A et al., 2023), it suggests that Col6 may be an important target for improving ventilator diaphragm dysfunction in diabetic mice.

We further performed GO and KEGG analyses to predict the function of DEGs. GO and KEGG enrichment analysis identified signaling pathways associated with VIDD in diabetic mice such as: signaling pathway, calcium signaling pathway, MAPK signaling pathway and AGE-RAGE signaling pathway in diabetic complications, etc (Figures 7D, E). In the analysis, we noticed that ECM was enriched, and it may be very closely related to VIDD in diabetic mice. Literature review found that extracellular matrix (ECM) is an important component of skeletal muscle. ECM accounts for 10% of skeletal muscle weight (Kjaer, 2004), and is located in the muscle at three levels: endomyuscular, perimuscular and epimuscular (de Rezende Pinto et al., 2015), in which a lot of collagen is distributed (Kovanen, 2012). As a special skeletal muscle, diaphragm has most of the characteristics of skeletal muscle (Zuo et al., 2000). In this study, we also found that there were different expressions of collagen in the diaphragms of different groups (Figures 7B, C). Studies have shown that ECM provides a frame structure for muscles, supporting muscle fibers, capillaries, and nerves. It plays an important role in the transmission, maintenance and repair of muscle fiber force (Gillies and Lieber, 2011; MAA, 2019). ECM deficiency can lead to muscular dystrophy or muscular atrophy (Schessl et al., 2006). In this study, the main components of ECM in DB mice decreased more significantly than C57 mice after mechanical ventilation, such as collagen, elastin and fibrillar protein, indicating that some components of ECM were insufficient or degraded too much during mechanical ventilation, resulting in diaphragmatic atrophy, which was manifested as more serious diaphragmatic dysfunction in DB mice.

5 Conclusion

In conclusion, our study provides a groundbreaking glimpse into transcriptional level changes in diaphragm function after MV in DB mice and C57 mice. Based on our results, ECM is an important focus of ventilator-associated diaphragm dysfunction in diabetic mice, providing clues for the further study of mechanical ventilation in diabetic mice. Col6 may be a promising target for diagnosis and treatment of ventilator diaphragmatic dysfunction in diabetic mice. Future research could delve into these aspects, driving a more complete understanding of the impact of diabetes on MV and ultimately guiding treatment innovation.

Data availability statement

The datasets presented in this study can be found in online repositories. The names of the repository/repositories and accession number(s) can be found below: <https://www.ncbi.nlm.nih.gov/sra/PRJNA1055679>.

Ethics statement

The animal study was approved by the Institutional Animal Care and Use Committee of Wuhan University. The study was conducted in accordance with the local legislation and institutional requirements.

Author contributions

RX: Formal Analysis, Investigation, Methodology, Writing—original draft. HY: Data curation, Formal Analysis, Investigation, Visualization, Writing—original draft. JY: Formal Analysis, Writing—original draft. RZ: Investigation, Writing—original draft. ZX: Formal Analysis, Writing—original draft. HM: Writing—review and editing. GL: Conceptualization, Formal Analysis, Visualization, Writing—review and editing. YZ: Conceptualization, Funding acquisition, Writing—review and editing.

Acknowledgments

The authors acknowledge the members of Emergency Center, Zhongnan Hospital of Wuhan University.

Conflict of interest

The authors declare that the research was conducted in the absence of any commercial or financial relationships that could be construed as a potential conflict of interest.

Publisher's note

All claims expressed in this article are solely those of the authors and do not necessarily represent those of their affiliated organizations, or those of the publisher, the editors and the reviewers. Any product that may be evaluated in this article, or claim that may be made by its manufacturer, is not guaranteed or endorsed by the publisher.

Supplementary material

The Supplementary Material for this article can be found online at: <https://www.frontiersin.org/articles/10.3389/fgene.2024.1387688/full#supplementary-material>

References

- Allamand, V., Bushby, K., and Consortium for Collagen VI-Related Myopathies (2010). 166th ENMC international workshop on collagen type VI-related myopathies, 22-24 May 2009, Naarden, The Netherlands. *166th ENMC Int. Workshop Collagen type VI-related Myopathies, 22-24 May 2009, Naarden, Neth. Neuromuscul Disord* 20 (5), 346–354. doi:10.1016/j.nmd.2010.02.012
- Anderson, J. C. (2015). Measuring breath acetone for monitoring fat loss: review. *Silver Spring, md.* 23 (12), 2327–2334. doi:10.1002/oby.21242
- Angelin, T. T., Sabatelli, P., Grumati, P., Bergamin, N., Golfieri, C., et al. (2007). Mitochondrial dysfunction in the pathogenesis of Ullrich congenital muscular dystrophy and prospective therapy with cyclosporins. *Proc. Natl. Acad. Sci. U. S. A.* 104 (3), 991–996. doi:10.1073/pnas.0610270104
- Azuelos, I., Jung, B., Picard, M., Liang, F., Li, T., Lemaire, C., et al. (2015). Relationship between autophagy and ventilator-induced diaphragmatic dysfunction. *Anesthesiology* 122 (6), 1349–1361. doi:10.1097/ALN.0000000000000656
- Bernardi, P., and Bonaldo, P. (2008). Dysfunction of mitochondria and sarcoplasmic reticulum in the pathogenesis of collagen VI muscular dystrophies. *Ann. N. Y. Acad. Sci.* 1147, 303–311. doi:10.1196/annals.1427.009
- Bonaldo, P., Zanetti, M., Piccolo, S., Volpin, D., and Bressan, G. M. (1998). Collagen VI deficiency induces early onset myopathy in the mouse: an animal model for Bethlem myopathy. *Hum. Mol. Genet.* 7, 2135–2140. doi:10.1093/hmg/7.13.2135
- Callahan La, S. G., and Supinski, G. S. (2014). Hyperglycemia-induced diaphragm weakness is mediated by oxidative stress. *Crit. Care* 18 (3), R88. doi:10.1186/cc13855
- Castagnaro, S., Cescon, M., and Bonaldo, P. (2021). Autophagy in the mesh of collagen VI. *Matrix Biol.* 100–101, 162–172. doi:10.1016/j.matbio.2020.12.004
- Cescon, M., Chen, P., and Bonaldo, P. (2015). Collagen VI at a glance. *J. Cell Sci.* 218 (19), 3525–3531. doi:10.1242/jcs.169748
- Chrisam, M., Castagnaro, S., Blaauw, B., Polishchuck, R., Cecconi, F., et al. (2015). Reactivation of autophagy by spermidine ameliorates the myopathic defects of collagen VI-null mice. *Autophagy* 11 (12), 2142–2152. doi:10.1080/15548627.2015.1108508
- Decramer, M., and Gayan-Ramirez, G. (2004). Ventilator-induced diaphragmatic dysfunction: toward a better treatment? *Am. J. Respir. Crit. Care Med.* 170 (11), 1141–1142. doi:10.1164/rccm.2409004
- de Rezende Pinto, W. B. V., de Souza, P. V. S., and Oliveira, A. S. (2015). Normal muscle structure, growth, development, and regeneration. *Curr. Rev. Musculoskelet. Med.* 8 (2), 176–181. doi:10.1007/s12178-015-9267-x
- Di Martino A, C. M., D'Agostino, C., Schilardi, F., Sabatelli, P., Merlini, L., et al. (2023). Collagen VI in the musculoskeletal system. *Int. J. Mol. Sci.* 24 (6), 5095. doi:10.3390/ijms24065095
- Fogarty, M. J., Mantilla, C. B., and Sieck, G. C. (2018). Breathing: motor control of diaphragm muscle. *Physiol. (Bethesda, Md.)* 33 (2), 113–126. doi:10.1152/physiol.00002.2018
- Gillies, A. R., and Lieber, R. L. (2011). Structure and function of the skeletal muscle extracellular matrix. *Muscle Nerve* 44 (3), 318–331. doi:10.1002/mus.22094
- Grumati, P., Sabatelli, P., Cescon, M., Angelin, A., Bertaggia, E., et al. (2010). Autophagy is defective in collagen VI muscular dystrophies, and its reactivation rescues myofiber degeneration. *Nat. Med.* 16 (11), 1313–1320. doi:10.1038/nm.2247
- Hafner, S., Frick, M., Dietl, P., and Calzia, E. (2014). Hyperglycemia, oxidative stress, and the diaphragm: a link between chronic co-morbidity and acute stress? *Crit. Care* 18 (3), 149. doi:10.1186/cc13913
- Heiskanen, M., Palotie, A., and Chu, M. L. (1995). Head-to-tail organization of the human Col6a1 and Col6a2 genes by fiber-fish. *Genomics* 29 (3), 801–803. doi:10.1006/geno.1995.9008
- Hessle, H., and Engvall, E. (1984). Type-vi collagen-studies on its localization, structure, and biosynthetic form with monoclonal-antibodies. *J. Biol. Chem.* 259 (6), 3955–3961. doi:10.1016/s0021-9258(17)43189-9
- Ichinoseki-Sekine, N., Smuder, A. J., Morton, A. B., Hinkley, J. M., Mor Huertas, A., and Powers, S. K. (2021). Hydrogen sulfide donor protects against mechanical ventilation-induced atrophy and contractile dysfunction in the rat diaphragm. *Clin. Transl. Sci.* 14 (6), 2139–2145. doi:10.1111/cts.13081
- Irwin, B. N., Sabatelli, P., Reggiani, C., Megighian, A., Merlini, L., et al. (2003). Mitochondrial dysfunction and apoptosis in myopathic mice with collagen VI deficiency. *Nat. Genet.* 35 (4), 367–371. doi:10.1038/ng1270
- Izzo, M. E., Riccardi, G., Della, P. G., and Della Pepa, G. (2021). A narrative review on sarcopenia in type 2 diabetes mellitus: prevalence and associated factors. *Nutrients* 13 (1), 183. doi:10.3390/nu13010183
- Keene, D. R., and Glanville, R. W. (1988). Ultrastructure of type-vi collagen in human-skin and cartilage suggests an anchoring function for this filamentous network. *J. Cell Biol.* 107 (5), 1995–2006. doi:10.1083/jcb.107.5.1995
- Kjaer, M. (2004). Role of extracellular matrix in adaptation of tendon and skeletal muscle to mechanical loading. *Physiol. Rev.* 84 (2), 649–698. doi:10.1152/physrev.00031.2003
- Kovanen, V. (2012). Intramuscular extracellular matrix: complex environment of muscle cells. *Exerc Sport Sci. Rev.* 30 (1), 20–25. doi:10.1097/00003677-200201000-00005
- Kuo, H. J., Keene, D. R., and Glanville, R. W. (1997). Type VI collagen anchors endothelial basement membranes by interacting with type IV collagen. *J. Biol. Chem.* 272 (42), 26522–26529. doi:10.1074/jbc.272.42.26522
- Lamadé, S. R., and Bateman, J. F. (2018). Collagen VI disorders: insights on form and function in the extracellular matrix and beyond. *Matrix Biol.* 71–72, 348–367. doi:10.1016/j.matbio.2017.12.008
- Leverve, X. (2003). Hyperglycemia and oxidative stress: complex relationships with attractive prospects. *Intensive Care Med.* 24 (9), 511–514. doi:10.1007/s00134-002-1629-3
- Liu, R., Li, G., Ma, H., Zhou, X., Wang, P., and Zhao, Y. (2021a). Transcriptome profiling of the diaphragm in a controlled mechanical ventilation model reveals key genes involved in ventilator-induced diaphragmatic dysfunction. *BMC Genomics* 22 (1), 472. doi:10.1186/s12864-021-07741-9
- Liu, R., Ma, H., Zhou, X., Wang, P., and Zhao, Y. (2021b). Transcriptome profiling of the diaphragm in a controlled mechanical ventilation model reveals key genes involved in ventilator-induced diaphragmatic dysfunction. *BMC Genomics* 22 (1), 472. doi:10.1186/s12864-021-07741-9
- Liu, Y.-Y., and Li, L.-F. (2018). Ventilator-induced diaphragm dysfunction in critical illness. *Exp. Biol. Med. (Maywood, N.J.)* 243 (17–18), 1329–1337. doi:10.1177/1535370218811950
- Maa, M. (2019). Skeletal muscle fibrosis: an overview. *Cell Tissue Res.* 375 (3), 575–588. doi:10.1007/s00441-018-2955-2
- Matecki, S., Dridi, H., Jung, B., Saint, N., Reiken, S. R., Scheuermann, V., et al. (2016). Leaky ryanodine receptors contribute to diaphragmatic weakness during mechanical ventilation. *Proc. Natl. Acad. Sci. U. S. A.* 113 (32), 9069–9074. doi:10.1073/pnas.1609707113
- Metti, S., Chrisam, M., La Spina, M., Baraldo, M., Braghetta, P., et al. (2021). Corrigendum: the polyphenol pterostilbene ameliorates the myopathic phenotype of collagen VI deficient mice via autophagy induction. *Front. Cell Dev. Biol.* 8, 615542. doi:10.3389/fcell.2020.615542
- Mrozek, S., Jung, B., Petrof, B. J., Pauly, M., Roberge, S., Lacampagne, A., et al. (2012). Rapid onset of specific diaphragm weakness in a healthy murine model of ventilator-induced diaphragmatic dysfunction. *Anesthesiology* 117 (3), 560–567. doi:10.1097/ALN.0b013e318261e7f8
- Nakai, H., Hirata, Y., Furue, H., and Oku, Y. (2023). Electrical stimulation mitigates muscle degradation shift in gene expressions during 12-h mechanical ventilation. *Sci. Rep.* 13 (1), 20136. doi:10.1038/s41598-023-47093-w
- Picard, M., Jung, B., Liang, F., Azuelos, I., Hussain, S., Goldberg, P., et al. (2012a). Mitochondrial dysfunction and lipid accumulation in the human diaphragm during mechanical ventilation. *Am. J. Respir. Crit. Care Med.* 186 (11), 1140–1149. doi:10.1164/rccm.201206-0982OC
- Picard, M., Liang, F., Azuelos, I., Hussain, S., Goldberg, P., et al. (2012b). Mitochondrial dysfunction and lipid accumulation in the human diaphragm during mechanical ventilation. *Am. J. Respir. Crit. Care Med.* 186 (11), 1140–1149. doi:10.1164/rccm.201206-0982OC
- Saeedi, P., Salpea, P., Malanda, B., Karuranga, S., Unwin, N., et al. (2019). Global and regional diabetes prevalence estimates for 2019 and projections for 2030 and 2045: results from the international diabetes federation diabetes atlas, 9th edition. *Diabetes Res. Clin. Pract.* 157, 107843. doi:10.1016/j.diabres.2019.107843
- Schessl, J., Bönnemann, C. G., and Bönnemann, C. G. (2006). Congenital muscular dystrophies and the extracellular matrix. *Semin. Pediatr. Neurol.* 13 (2), 80–89. doi:10.1016/j.spen.2006.06.003
- Schmittgen, T. D., and Livak, K. J. (2008). Analyzing real-time PCR data by the comparative C(T) method. *Nat. Protoc.* 3 (6), 1101–1108. doi:10.1038/nprot.2008.73
- Starace, M., Bruni, F., Quadrelli, F., Cedirian, S., Baraldi, C., et al. (2023). Alopecia in patients with collagen VI-related myopathies: A novel/unrecognized scalp phenotype. *Int. J. Mol. Sci.* (24), 7. doi:10.3390/ijms24076678
- Van Lunteren, E., and Moyer, M. (2013). Gene expression of sternohyoid and diaphragm muscles in type 2 diabetic rats. *BMC Endocr. Disord.* 13, 43. doi:10.1186/1472-6823-13-43

Wang, Y., and Pessin, J. E. (2013). Mechanisms for fiber-type specificity of skeletal muscle atrophy. *Curr. Opin. Clin. Nutr. Metabolic Care* 16 (3), 243–250. doi:10.1097/MCO.0b013e328360272d

Weil, D., Passage, E., N'Guyen, V. C., Pribulaconway, D., Mann, K., et al. (1988). Cloning and chromosomal localization of human genes encoding the three chains of type VI collagen. *Am. J. Hum. Genet.* 42 (3), 435–445.

Yan, Z., Okutsu, M., Akhtar, Y. N., and Lira, V. A. (2011). Regulation of exercise-induced fiber type transformation, mitochondrial biogenesis, and angiogenesis in skeletal muscle. *J. Appl. Physiology (Bethesda, Md, 1985)* 110 (1), 264–274. doi:10.1152/jappphysiol.00993.2010

Yasuda, T., Ishihara, T., Ichimura, A., and Ishihara, N. (2023). Mitochondrial dynamics define muscle fiber type by modulating cellular metabolic pathways. *Cell Rep.* 42 (5), 112434. doi:10.1016/j.celrep.2023.112434

Zhu, E., and Sassoon, C. S. H. (2012). Ventilator-induced diaphragmatic vascular dysfunction. *Crit. Care Med.* 40 (10), 2914–2915. doi:10.1097/CCM.0b013e318263236e

Zuo, L., Wright, V. P., Liu, C. Y., Merola, A. J., Berliner, L. J., et al. (2000). Intra- and extracellular measurement of reactive oxygen species produced during heat stress in diaphragm muscle. *Am. J. Physiol. Cell Physiol.* 279 (4), C1058–C1066. doi:10.1152/ajpcell.2000.279.4.C1058